

Simulations of Beam-Beam Interaction for Round Beams

A.A. Valishev

Budker Institute of Nuclear Physics, Novosibirsk, 630090, Russia

In this paper we summarize the results of numerical simulations of beam-beam interaction in electron-positron collider with round beams. A particular case of the VEPP-2000 collider [1] was studied using both strong-strong and weak-strong models. For the latter, two simulation codes are compared showing similar results. Based on the simulations, the collider optics is chosen which is expected to provide the design luminosity.

1. INTRODUCTION

Effects arising from electromagnetic interaction of colliding bunches, the so-called beam-beam effects, limit the maximum attainable luminosity of modern circular electron-positron colliders. For the case of equal parameters of the bunches the luminosity can be expressed by the formula

$$L = \frac{\pi \gamma^2 \xi_x \xi_y \varepsilon_x f}{r_e^2 \beta_y^*} \left(1 + \frac{\sigma_y}{\sigma_x} \right)^2,$$

where γ is the relativistic factor, r_e is the classical electron radius, f is the frequency of collisions, β_y^* is the betatron function at the Interaction Point (IP), σ_x and σ_y are the horizontal and vertical r.m.s. beam sizes at IP, ε_x is the horizontal beam emittance and ξ_x , ξ_y are the beam-beam parameters. The dimensionless beam-beam parameters represent linearized betatron tune shift caused by the interaction and are related to the particle density at the collision point [2].

With fixed machine parameters (γ , β_y^* , and ε_x) higher luminosity can be achieved by utilizing two factors: by increasing the collision frequency, e.g. with multibunch regime; and by increase of the attainable beam-beam parameters. The first way is hard to implement at machines with small circumference because of parasitic collisions. On the other hand, the highest beam-beam parameters at present colliders do not exceed 0.09. The limitation is believed to be caused by beam-beam driven nonlinear effects in beam dynamics. The electromagnetic force from the counter bunch is highly nonlinear. Being localized in azimuth it drives nonlinear betatron coupling resonances. At some threshold beam intensity these resonances overlap, leading to beam size blow-up and degradation of the beam life time detrimental to luminosity and background conditions of the experiment.

Various methods are proposed to overcome this limit. One of them is the idea of Round Colliding Beams. The first straightforward advantage of round beams is that ξ_x is equal to ξ_y and the cross-section of beams at the IP is round. This geometric property gives at least a factor of two increase in luminosity at constant ξ [2].

But the main idea of the method is aimed at enhancement of the maximum attainable beam-beam parameter. This can be achieved because of elimination of

the betatron coupling resonances by introducing an additional integral of motion, namely the longitudinal component of the particle's angular momentum [3,4]. Analytical models show the possibility to construct an integrable optics and predict the advantage of the round beams [4]. Some experimental tests of a Mobius accelerator [5] which is an option of round beam machine, were done at CESR (Cornell, USA) demonstrating accessibility of the beam-beam parameter as high as 0.1 [6]. However, the round beams in high luminosity regime were not obtained to this moment.

The collider VEPP-2000 (BINP, Novosibirsk) with the design luminosity of $1 \times 10^{32} \text{ cm}^{-2} \text{ s}^{-1}$ at 1 GeV per beam will use round beams as one of its operation options, thus presenting an opportunity to check the method. The design goal of the beam-beam parameter for the round beam option is 0.1.

In the past decade a number of computer codes appeared [7,8,9] using advanced models of the beam-beam interaction and allowing to perform numerical simulations of colliding bunches with sufficient accuracy. Although the computer simulations do not reproduce the experimental results precisely, they give a good answer about the main characteristics of the system: beam size and the beam-beam limit, coherent beam-beam tune shift, etc. Thus, a comprehensive numerical simulation of beam-beam effects for a new collider is highly advisable.

We used two tracking codes to simulate the beam-beam effects in VEPP-2000. The first one is the modified strong-strong Particle In Cell (PIC) code BBSS which has been initially developed for KEKB [7]. This code was also used in weak-strong mode for comparison with LIFETRAC [10].

Previous studies have shown strong dependence of the beam-beam phenomena in the round beam on the nonlinear betatron dynamics, e.g. due to sextupoles [11]. Hence, the beam-beam problem for VEPP-2000 was studied together with the choice of main optical parameters: betatron function at the interaction point, working point, sextupole chromaticity correction scheme.

In this paper we present the results of simulation of beam-beam interaction for the VEPP-2000 optics using weak-strong and strong-strong models. The calculations show availability of very high values of ξ in ideal optics and reveal some problems in a more realistic case. Based on this simulation, a corrected machine optics has been chosen.

Section 2 describes optics and lists parameters of the VEPP-2000 collider, in Sec. 3 the weak-strong simulation

results are reported, Sec. 4 presents the strong-strong case, and Sec. 5 gives a summary of the results.

2. COLLIDER PARAMETERS

VEPP-2000 design consists of two symmetrical arcs with two diametrically opposite symmetrical Interaction Points (Fig. 1). Each arc is constructed of two mirror double bend achromats. Two straight sections between the achromats are occupied with the RF cavity and beam injection system. Focusing in the interaction regions is done by superconducting solenoids located on both sides of the IP. Besides focusing the solenoids rotate the transverse betatron modes by $\pm \pi/4$. This is true when the requirement

$$\int_0^l B_z ds = \frac{1}{2} \oint B_y ds$$

is fulfilled, where B_z is the longitudinal magnetic field in the solenoid and integration is done over the solenoid length l , and B_y is the guiding vertical magnetic field. The sign of the rotation is determined by the sign of B_z which is marked by direction of arrows in Fig. 1.

In the main regime (labeled “normal” round in Fig. 1) the transverse betatron modes are rotated by the final focus solenoids by $+\pi/2$ in one IP and by $-\pi/2$ in another which results in equal emittances. Indeed, the mode which is horizontal in one arc and excited by quantum fluctuations of synchrotron radiation becomes vertical in the second arc and vice versa. Since the arcs are symmetrical the modes are excited equally which yields equal emittances.

Solenoids have separate power supplies and can be switched in a number of ways. For example, when solenoids on the sides of each IP have opposite polarities the angle of rotation is zero which is the case of conventional flat beam machine. In this regime the horizontal emittance is twice the mode emittance of the “normal” mode and vertical emittance is excited only via residual betatron coupling. Another possibility is the so-called Mobius machine, when the betatron oscillation plane is rotated by π each turn.

Requirement of conservation of the longitudinal component of the particle’s angular momentum results in equal β^* -functions and fractional betatron tunes.

In VEPP-2000 electrons and positrons move in common vacuum chamber and both beams contain 1 bunch. Maximum operation energy is 1 GeV per beam but all simulations were carried out at injection energy of 0.9 GeV. Table 1 shows the parameters of VEPP-2000 which resulted from optimization.

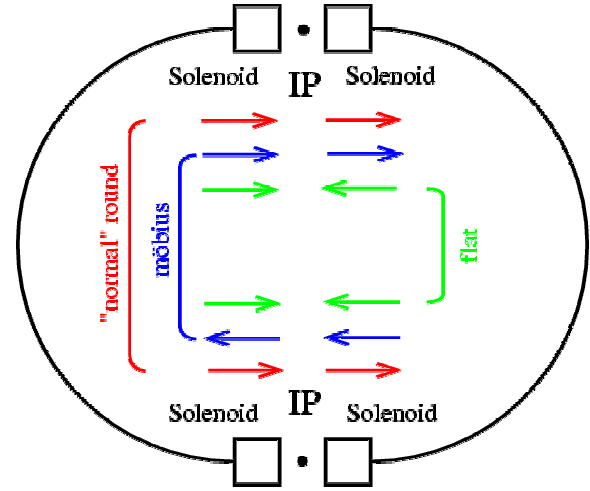


Figure 1. Scheme of the VEPP-2000 collider.

Parameter	Value
Beam energy	1 GeV
Circumference	24.38 m
RF frequency	172 MHz
RF voltage	0.1 MV
RF harmonic	14
Momentum compaction	0.036
Synchrotron tune	0.0035
Energy spread	6.4×10^{-4}
Beam emittances (x,y)	1.29×10^{-7} m rad
Dimensionless damping decrements (x,y,z)	2.19×10^{-5} 2.19×10^{-5} 4.83×10^{-5}
Betatron tunes	4.05, 2.05
Betatron functions @ IP	10 cm
Particles per bunch	1×10^{11}
Beam-beam parameter (x,y)	0.1, 0.1
Luminosity per IP	$1 \times 10^{32} \text{ cm}^{-2} \text{ s}^{-1}$

Table 1. Main parameters of VEPP-2000.

3. WEAK-STRONG CASE

In the so-called weak-strong model two colliding bunches have different intensities and distribution function of the stronger bunch is regarded to be unchanged by the interaction. This completely excludes effects involving coherent motion of bunches but dramatically eases calculations and makes them faster. We have at our disposal a well tested weak-strong code LIFETRAC by Shatilov [10]. The main features of this code are:

- the code is fully 3-Dimensional
- allows machine lattice with sextupole and octupole nonlinearities
- takes full account of the radiation excitation and damping
- contains advanced technique for calculation of the beam life time.

A strong-strong code can be run in the weak-strong mode by simply making the beam intensities significantly different. We used this possibility to benchmark LIFETRAC and BBSS in weak-strong mode against each other.

Figure 2 presents results of calculations in the ideal VEPP-2000 lattice without nonlinearities. The simulation does not display emittance blow-up up to the beam-beam parameter value of 0.2 and increase of the emittance is compensated by the dynamical beta shrinking resulting in constant beam size.

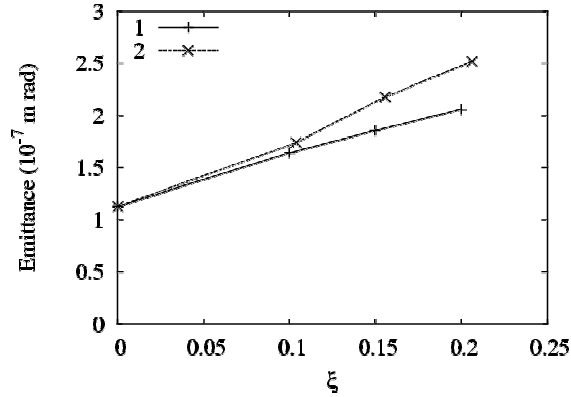


Figure 2. Emittance of the weak beam vs. the beam-beam parameter in linear lattice. 1 - LIFETRAC, 2 - BBSS in weak-strong mode.

Consideration of nonlinear lattice changes the situation. While the beam core remains stable some particles drift to larger amplitudes giving rise to the beam tails (Fig. 3). As the result, particle losses occur at dynamical aperture and the beam life time is decreased at ξ values of 0.15 for LIFETRAC and 0.12 for BBSS.

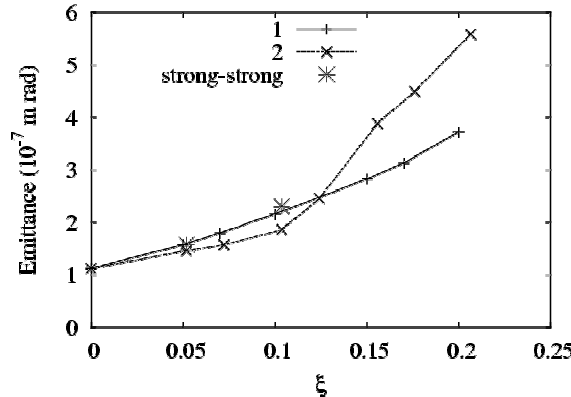


Figure 3. Emittance of the weak beam vs. the beam-beam parameter with sextupoles. 1 - LIFETRAC, 2 - BBSS in weak-strong mode.

Comparison of the codes gives good agreement. At moderate ξ 's the simulated emittances do not differ, while at high values of the beam-beam parameter BBSS exhibits bigger beam blow-up (Fig. 2). The same situation is seen in Fig. 3, where a similar comparison is shown with chromaticity correction sextupoles switched on. This

difference can be explained by the three dimensional (3-D) effects which are excluded in the quasi weak-strong calculation (BBSS) since we did not utilize longitudinal bunch slicing in it and the weak beam was infinitely thin. Although the ratio of the bunch length σ_z and β^* is 0.25, the hourglass effect might act on the interaction. To prove this statement a comparison was done with thin bunch in the both codes. Results presented in Figs. 4, 5 reveal reduced discrepancy.

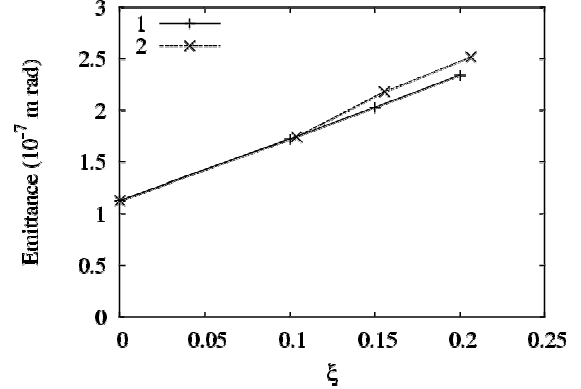


Figure 4. Emittance of the weak-beam vs. the beam-beam parameter in linear lattice. 1 - LIFETRAC in quasi 2-D mode, 2 - BBSS in weak-strong mode.

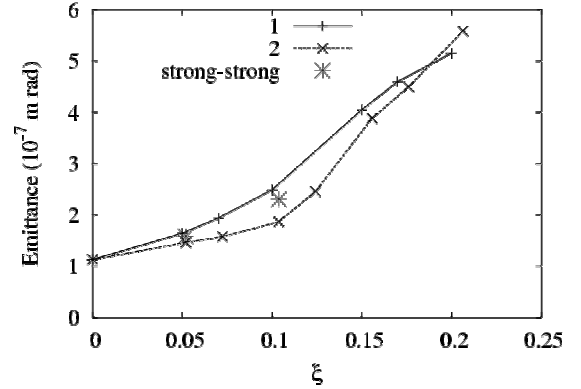


Figure 5. Emittance of the weak beam vs. the beam-beam parameter with sextupoles. 1 - LIFETRAC in quasi 2-D mode, 2 - BBSS in weak-strong mode.

4. STRONG-STRONG CASE

4.1. The Code

The strong-strong case presupposes solution of self-consistent problem for the system of two colliding beams. This model is more realistic compared to the weak-strong one but at the same time more difficult to implement and requires considerable computer resources. The computer code BBSS developed at KEK by Ohmi shows good agreement with experimental data for KEKB. It is described in detail in [3].

The code for calculating the beam-beam force did not need modification for our purposes. Here we describe only the main features of the algorithm.

Each colliding beam is represented with N_p macroparticles forming a 3-dimensional distribution in space, where N_p is taken big enough to avoid statistical effects and in our case was 5×10^4 .

The code uses 2-D mesh to evaluate the transverse field which is calculated via the Poisson equation using Fast Fourier Transformation (FFT). Particles of the opposite bunch are tracked through the field. We used 128×128 mesh with coordinate region covered approximately ± 10 of the transverse beam σ . Due to a comparatively long radiation damping time in VEPP-2000 (5×10^4 turns) we did not use longitudinal slicing of the beam, hence the beam-beam interaction was substantially 2-dimensional.

Modifications of the code concern particle tracking over the accelerator arc and radiation damping/quantum excitation. Nonlinearities of the machine optics are known to influence the beam-beam effect, therefore we included the chromaticity correction sextupoles as thin elements with linear transformations of betatron coordinates between them (Fig. 6). Simulated dynamical aperture in the absence of beam-beam interaction reproduces very well the results of special codes.

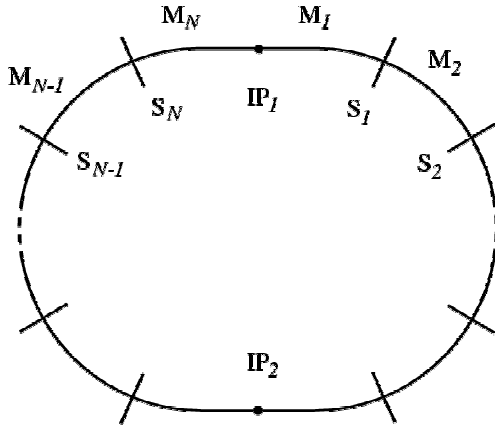


Figure 6. Schematic representation of the arc tracking.

Another important effect for electron machines consists in dynamical change of the beam emittance due to deformation of the machine lattice by linear part of the beam-beam force. In the original code the equilibrium emittance was simulated by applying radiation damping and random quantum excitation once per turn:

$$X = \lambda X_0 + \sqrt{(1 - \lambda^2)} \mathcal{E} \cdot \vec{r}.$$

Here X is 2-vector of dynamic variables of one normal mode, $\lambda = e^{-\delta}$ with δ being the damping decrement, \mathcal{E} is the nominal equilibrium beam emittance, and \vec{r} is a vector of two Gaussian random numbers with the mean value equal to 0 and $\sigma = 1$. To apply this mapping one needs to transform the particle's betatron coordinates to the normal basis after each turn which slows down the computation. Moreover, it did not give the correct deformation of the beam emittance. To repair it, we introduced the modified mapping

$$\vec{x} = (I + D)\vec{x}_0 + \tilde{B}\vec{r}_6$$

which is applied to 6-vector \vec{x} of physical coordinates after each section of the arc transformation consisting of linear mapping M_i and sextupole s_i . Here I is 6×6 identity matrix, D is the damping part of the transfer matrix for the i -th section [12], and \tilde{B} is the excitation correlation matrix computed as follows [13].

The integrated diffusion matrix \bar{B} [12] can be calculated using the SAD code [14]. Next, the J matrix is introduced as $J = \bar{B}S$ where S is the 6×6 symplectic matrix. Using the eigenvectors Y and eigenvalues ν of J

$$JY_j = \bar{B}SY_j = i\nu_j Y_j, \quad j = 1 \dots 3,$$

one can decompose \bar{B} :

$$\bar{B} = \sum_{j=1}^3 \nu_j \Re[Y_j \otimes Y_j^{*T}].$$

The random excitation vector will be given by the correlation matrix

$$\tilde{B} = \left\{ \sqrt{\epsilon_1} \Re Y_1, \sqrt{\epsilon_1} \Im Y_1, \sqrt{\epsilon_2} \Re Y_2, \sqrt{\epsilon_2} \Im Y_2, \sqrt{\epsilon_3} \Re Y_3, \sqrt{\epsilon_3} \Im Y_3 \right\}^T$$

multiplied by the random 6-vector \vec{r}_6 .

Figures 7 and 8 show comparison of tracking using weak-strong linearized beam-beam interaction and the modified quantum excitation with calculation using conventional optics code, namely, SAD [14]. In SAD, the axisymmetric beam-beam lens was modeled using a pair of thin solenoids placed at the IP.

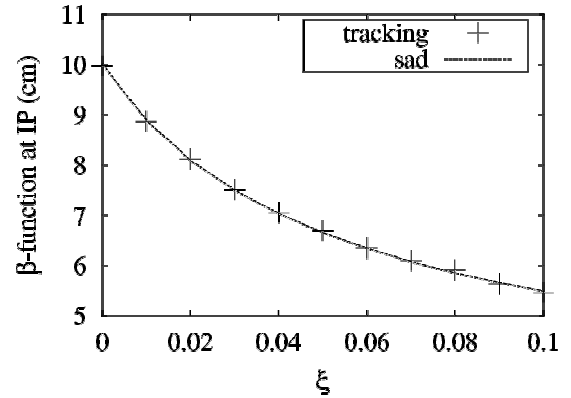


Figure 7. Beta function vs. ξ . Weak-strong linearized beam-beam interaction.

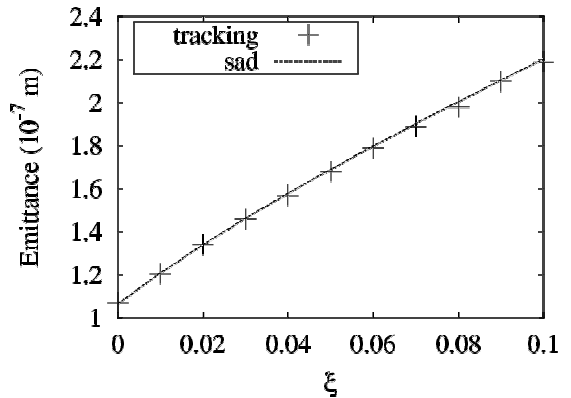


Figure 8. Weak beam emittance vs. ξ . Weak-strong linearized beam-beam interaction.

4.2. Simulation Results

Initial design parameters were $\beta^* = 6.3$ cm, $\varepsilon = 2.2 \times 10^{-7}$ m rad and fractional betatron tune $Q = 0.1$. Simulation without sextupoles has shown that values of ξ as high as 0.15 can be reached without degradation of luminosity (Fig. 9). The spectrum of dipole oscillations with infinitesimally small amplitude (Fig. 10) is clean, showing no lines except the expected σ and π modes (the tune shift is twice the ξ due to two IPs).

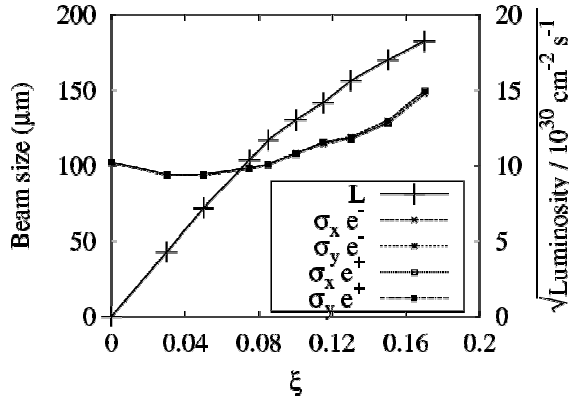


Figure 9. Beam size at IP and square root of the luminosity per 1 IP vs. the nominal beam-beam parameter. Linear collider optics.

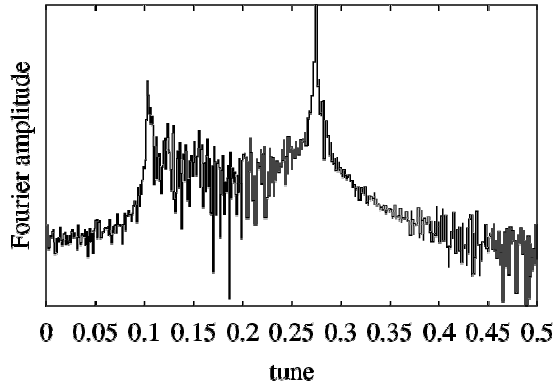


Figure 10. Fourier spectrum of the transverse dipole signal at $\xi = 0.17$ (logarithmic scale).

However, this optics has limited aperture, both dynamical and physical which is limited in the solenoids of the final focus. Although the beam size growth (Fig. 11) is not very large as compared, for example, with the flat-beam collision, particle losses arise at rather moderate values of ξ (0.06-0.07, Fig. 14). Apparently, this happens because of 'shrinking' of the dynamical aperture in the optics distorted by the beam-beam force. This was justified by tracking simulation using SAD, where the dynamical aperture of the distorted lattice was as low as 5σ at $\xi = 0.05$ (Fig. 12).

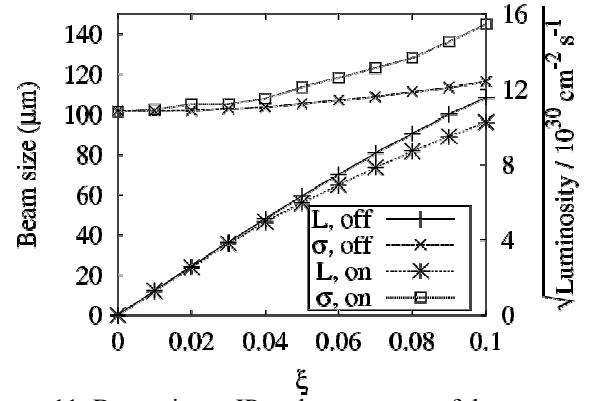


Figure 11. Beam size at IP and square root of the luminosity vs. ξ . Comparison of linear lattice and optics with sextupoles for $\beta^* = 6.3$ cm.

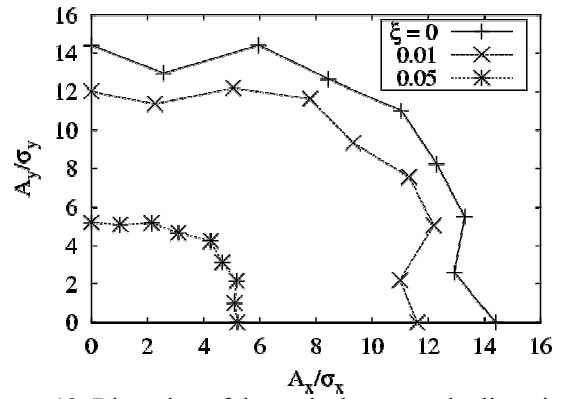


Figure 12. Distortion of dynamical aperture by linearized beam-beam interaction simulated with SAD for $\beta^* = 6.3$ cm optics.

This problem initiated the search of new optics aimed at increasing the aperture. Increasing of the β^* value from 6.3 to 10 cm with simultaneous reduction of the beam emittance allows to conserve the beam size at IP and luminosity at constant bunch population. The betatron tune was changed to 0.05. Together with improvement of the phase relations between sextupoles this resulted in enhancement of the aperture (Fig. 13) and elimination of particle losses up to $\xi = 0.11$ (Fig. 14). Figure 15 shows the simulated dependence of the beam size and luminosity on the nominal beam-beam parameter for the new optics.

Simulations show that the system maintains stability when moderate distortions of the optics are applied, for example 5% difference between β_x^* and β_y^* does not lead to qualitative change of the beams behavior.

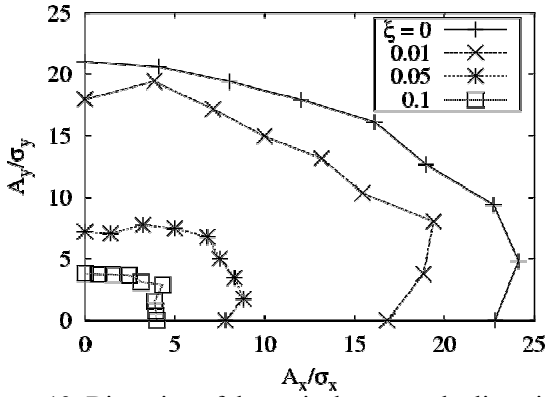


Figure 13. Distortion of dynamical aperture by linearized beam-beam interaction simulated with SAD for $\beta^* = 10$ cm optics.

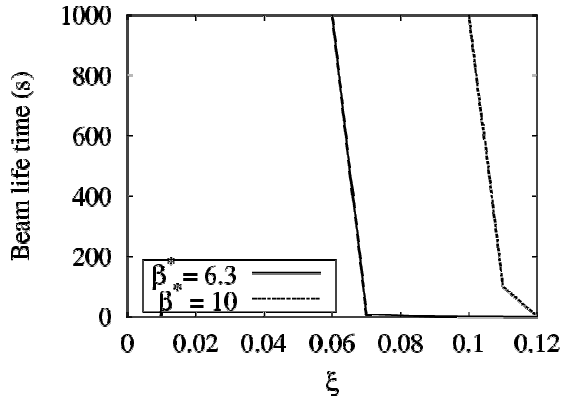


Figure 14. Simulated beam life time vs. the beam-beam parameter.

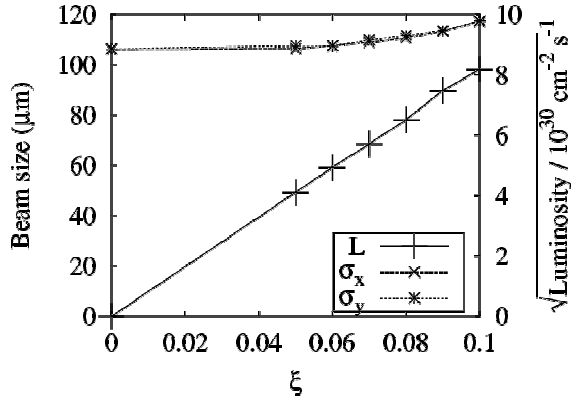


Figure 15. Beam size at IP and the luminosity vs. the beam-beam parameter for the $\beta^* = 10$ cm optics.

Betatron tune scan (Fig. 16) revealed that operation with the tune in the range from 0.05 to 0.09 is possible, while at tunes higher than 0.1 coherent oscillations develop, both of dipole and quadrupole symmetry. As an example, the evolution of the dipole moment with time at $Q = 0.05$ and $Q = 0.13$ for $\xi = 0.05$ is plotted in Figs. 17 and 18, correspondingly. In Fig. 18 the beams display dipole oscillations with amplitudes up to 1.5 of the beam size. Spectral analysis shows that the antisymmetric π mode is

unstable. After development of the instability the coherence is lost and the oscillations are damped, causing the beams to shrink to their original size which in turn causes the situation to repeat. Nature of this effect is not well understood at this moment. A more elaborate analysis involving 3-D simulations is required to clarify the problem.

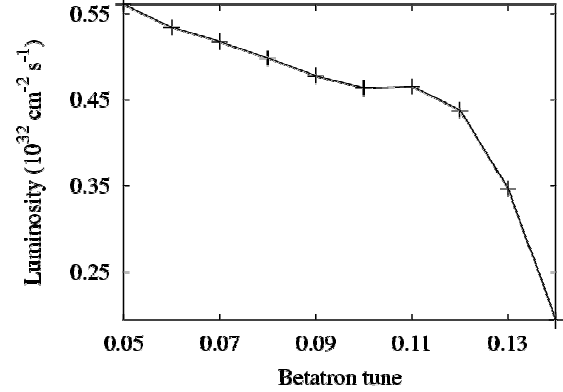


Figure 16. Dependence of the luminosity on fractional betatron tune.

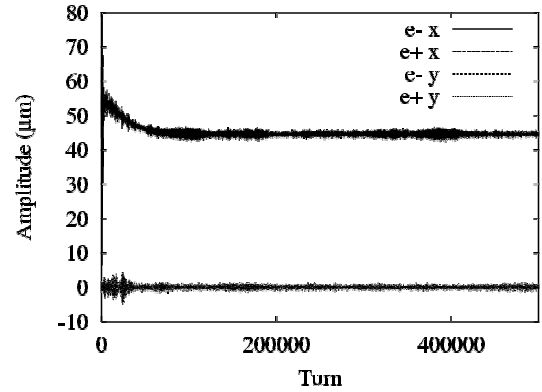


Figure 17. Evolution of the beam dipole moments. $Q = 0.05$ and $\xi = 0.05$.

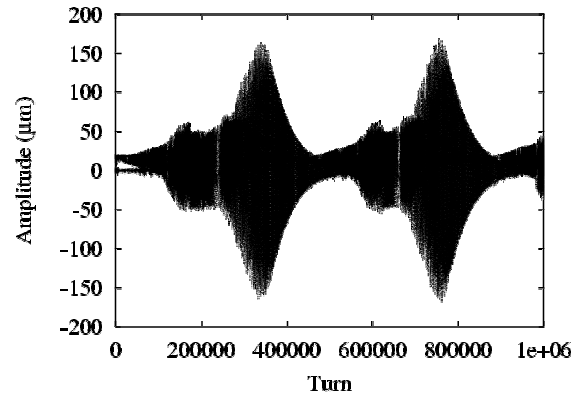


Figure 18. Evolution of the beam dipole moments. $Q = 0.13$ and $\xi = 0.05$.

5. SUMMARY AND OUTLOOK

Simulation of beam-beam effects for round colliding beams at the VEPP-2000 collider using both the strong-strong 2-D PIC code and 3-D weak-strong code predicts values of the maximum attainable beam-beam parameter up to at least 0.15 in a lattice without nonlinearities. Comparison of two weak-strong codes revealed good agreement of results.

Limitation of the transverse dynamical aperture caused by machine nonlinearities represented by chromaticity correction sextupoles leads to the beam life time degradation which is not however accompanied by the size blow-up. A new optics of VEPP-2000 has been developed to increase the dynamic aperture. Simulation for the new optics does not show particle losses up to $\xi=0.1$ which allows to reach the design luminosity.

2-dimensional strong-strong simulation displays coherent instability at fractional betatron tunes higher than 0.1.

Future efforts are required to enhance the strong-strong simulation to 3-dimensional case, and a more elaborate mapping through solenoids including the edge cubic nonlinearity is needed since it is believed to influence the dynamical aperture.

Acknowledgments

The author is grateful to E. Perevedentsev and Prof. Yu. Shatunov for attention and fruitful discussions. The author is indebted to Prof. K. Ohmi and D. Shatilov for the simulation codes.

Work supported by Grant of President of Russian Federation MK-1722.2003.02 and ISTC Grant 1928.

References

- [1] Yu.M. Shatunov *et al.*, in *Proceedings of the 7th European Particle Accelerator Conference, Vienna, 2000*, (Austrian Academy of Sciences Press, Vienna, 2000), p. 439
- [2] Yu.M. Shatunov, *Frascati Physics Series Vol. X*, p. 49 (1998)
- [3] V.V. Danilov *et al.*, in *Proceedings of the 5th European Particle Accelerator Conference, Barcelona, 1996*, (IOP, Bristol, 1996), Vol. 2, p. 1149
- [4] V.V. Danilov and E.A. Perevedentsev, *Frascati Physics Series Vol. X*, p. 321 (1998)
- [5] R. Talman, *Phys. Rev. Lett.* **74**, 1590 (1995)
- [6] E. Young *et al.*, in *Proceedings of the 17th Particle Accelerator Conference, Vancouver, Canada, 1997*, (IEEE, Piscataway, NJ, 1998), Vol. 2, p. 1542
- [7] K. Ohmi, *Phys. Rev. E* **59**, 7287 (2000)
- [8] S. Krishnagopal, *Phys. Rev. Lett.* **76**, 235 (1996)
- [9] Y. Cai *et al.*, *Phys. Rev. ST Accel. Beams* **4**, 011001 (2001)
- [10] D. Shatilov, *Part. Accel.* **52**, 65 (1996)
- [11] I. Nesterenko, D. Shatilov, and E. Simonov, in *Proceedings of the 17th Particle Accelerator Conference, Vancouver, Canada, 1997*, (IEEE, Piscataway, NJ, 1998), Vol. 2, p. 1762
- [12] K. Ohmi, K. Hirata, and K. Oide, *Phys. Rev. E* **49**, 751 (1994)
- [13] E. Perevedentsev (private communication)
- [14] <http://acc-physics.kek.jp/SAD/sad.html>